



Universiteit  
Leiden  
The Netherlands

## Single cell biochemistry to visualize antigen presentation and drug resistance

Griekspoor, A.C.

### Citation

Griekspoor, A. C. (2006, November 1). *Single cell biochemistry to visualize antigen presentation and drug resistance*. Retrieved from <https://hdl.handle.net/1887/4962>

Version: Corrected Publisher's Version

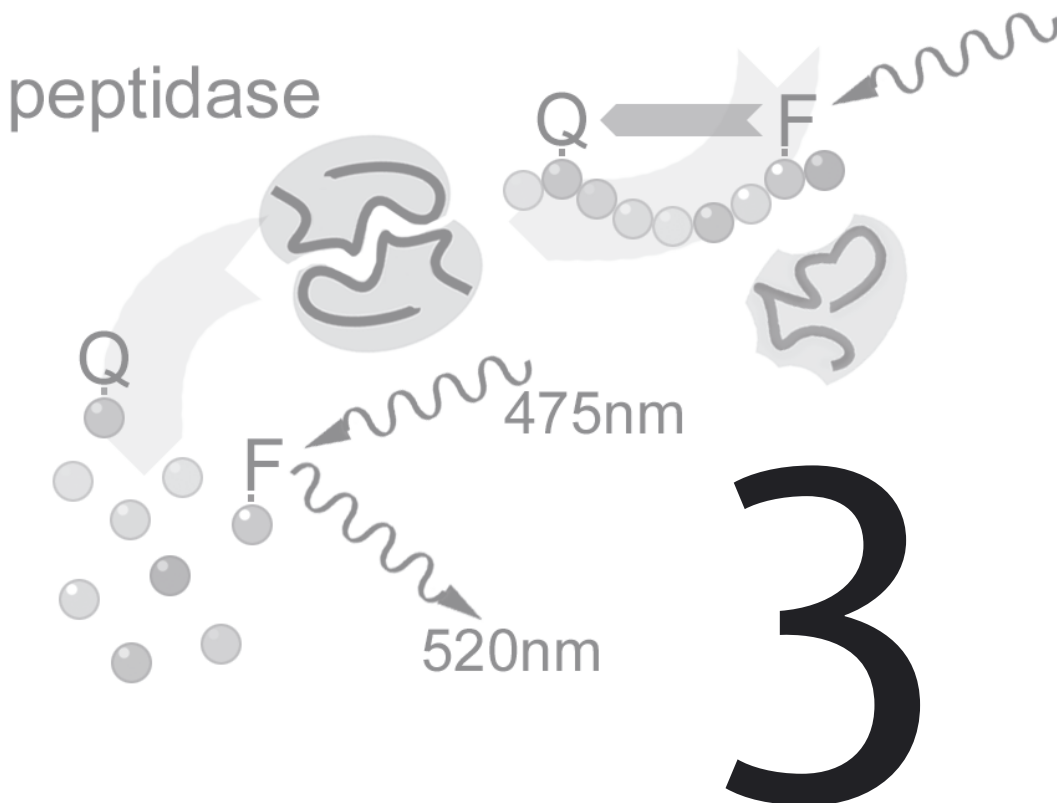
License: [Licence agreement concerning inclusion of doctoral thesis in the Institutional Repository of the University of Leiden](#)

Downloaded from: <https://hdl.handle.net/1887/4962>

**Note:** To cite this publication please use the final published version (if applicable).

# Peptide Diffusion, Protection, and Degradation in Nuclear and Cytoplasmic Compartments before Antigen Presentation by MHC Class I

Reprinted from *Immunity*, vol. 18: 97–108,  
Copyright (2003), with permission from Elsevier





# Peptide Diffusion, Protection, and Degradation in Nuclear and Cytoplasmic Compartments before Antigen Presentation by MHC Class I

Eric Reits<sup>1</sup>†, Alexander Griekspoor<sup>1</sup>, Joost Neijssen<sup>1</sup>, Tom Groothuis<sup>1</sup>, Kees Jalink<sup>1</sup>, Peter van Veelen<sup>2</sup>, Hans Janssen<sup>1</sup>, Jero Calafat<sup>1</sup>, Jan Wouter Drijfhout<sup>2</sup>, and Jacques Neefjes<sup>1</sup>

<sup>1</sup>Division of Tumour Biology and Cell Biology, The Netherlands Cancer Institute, Amsterdam, The Netherlands.

<sup>2</sup>Department of Immunohematology and Blood Transfusion, Leiden University Medical Centre, Leiden, The Netherlands

Antigenic peptides generated by the proteasome have to survive a peptidase-containing environment for presentation by MHC class I molecules. We have visualized the fate and dynamics of intracellular peptides in living cells. We show that peptides are distributed over two different but interconnected compartments, the cytoplasm and the nucleus, and diffuse rapidly through and between these compartments. Since TAP is excluded from the nuclear face of the nuclear envelope, nuclear peptides have to leave the nucleus to contact TAP. Thereby, these peptides encounter cytosolic peptidases that degrade peptides within seconds unless bound to chromatin. Since peptide degradation is far more efficient than translocation, many peptides will be lost for antigen presentation by MHC class I molecules.

## Introduction

The rate and specificity of the various steps in the antigen-processing pathway determine the outcome of a MHC class I-restricted response. Many peptides presented by MHC class I molecules are derived from newly synthesized proteins, but ultimately all intracellular proteins will be degraded into peptides and finally into amino acids (1, 2). The proteasome is the major proteolytic complex involved in the generation of peptides from intracellular proteins (3). Proteasomes can generate peptides that are N-terminally extended, and further trimming by aminopeptidases is then required to fit MHC class I molecules (4). Peptides can be trimmed to the correct

size for binding to MHC class I molecules by ER peptidases (5, 6), but many peptides will transiently bind to various ER chaperones before removal from the ER lumen by the Sec61p translocon (7). After returning to the cytoplasm, peptides can be further trimmed by cytoplasmic peptidases and again attempt to associate with MHC class I until they are too small to be recognized by TAP (8).

Although most players in the process of MHC class I antigen presentation are known, their kinetic relationship is unclear. Only a small percentage of peptides generated will be able to stably bind MHC class I molecules, and it is unclear why most peptides fail to bind MHC class I. A large fraction of peptides may be lost for antigen presentation (6, 9, 10). Various cytoplasmic peptidases may be involved both in gener-

## CORRESPONDENCE

Jacques J. Neefjes  
Division of Tumour Biology  
The Netherlands Cancer  
Institute  
Plesmanlaan 121  
1066 CX Amsterdam  
The Netherlands  
Tel.: +31 20 512 2012  
Fax: +31 20 512 2029  
E-mail: j.neefjes@nki.nl

*Immunity* 2003  
Vol. 18: 97-108

Copyright © Cell Press 2003

† Present address: Department of Cell Biology and Histology, Amsterdam Medical Center, The Netherlands.

ating the correct epitopes from extended peptides and in full degradation of these peptides. *In vitro* experiments have revealed that cytoplasmic peptidases like tripeptidyl peptidase II (TPPII) (11), leucine aminopeptidase (LAP) (12), and thimet oligopeptidase (TOP) (4) are able to degrade peptides with different specificities. While TPPII removes N-terminal tripeptides stepwise from unblocked oligopeptides, LAP removes single hydrophobic amino acids from the N-terminus. The expression of some of these peptidases is controlled by interferon  $\gamma$  (12), suggesting that they influence the pool of peptides presented by MHC class I. It is unclear how the heterogeneous peptidase pool affects the outcome of MHC class I-restricted antigen presentation. In fact, even for the few cytoplasmic peptidases known to date, their relative expression levels and activities have not been defined. TAP may compete with cytoplasmic peptidases for peptide substrates, but peptides could also be protected against immediate degradation if proteasomes would associate directly with TAP or if peptides bind to cytoplasmic/nuclear chaperones immediately after production by the proteasome. The heat shock proteins hsp70 and hsp90 are thought to protect peptides against peptidase activity by shuttling them through the cytoplasm (13). However, there is no direct *in vivo* evidence that protection by chaperones occurs during peptide transfer from the proteasome to the TAP transporter, nor is there any evidence for a direct interaction between the proteasome and TAP. Alternatively, peptides may contact TAP by simple diffusion. The efficiency of MHC class I antigen presentation would then depend on peptide dynamics and intracellular peptidase activity.

Using fluorescent probes, we here describe the fate of intracellular peptides in living cells. Our data uncovers novel steps in the process of antigen processing and presentation. We show that peptides are distributed over two different but interconnected compartments, the cytoplasm and the nucleus. Nuclear peptides have to leave the nucleus to contact TAP but then encounter various peptidases like LAP and TPPII, which are not present in the nucleus. Many peptides destined for MHC class I loading are targeted by cytosolic peptidases, as overexpression of the peptidase LAP limits peptide loading of MHC class I molecules. Fluorescent peptides compete with endogenous peptides in the nuclear compartment for binding to chromatin, which decreases the rate of degradation. This could be important during mitosis as peptides generated from proteins expressed during the cell cycle would

be preserved for antigen presentation by binding to chromatin. Although peptides move fast, the rate of degradation allows them to move only once through a cell before being degraded. Since peptides only have a limited time to find TAP, most peptides will be lost for antigen presentation by MHC class I molecules.

## Experimental Procedures

### Cell Lines, DNA Constructs, and Immunostaining

The human melanoma cell line Mel JuSo stably transfected with TAP1-GFP has been described before (1). LMP2-GFP expressing Mel JuSo cells were generated as described (14). Mel JuSo cells were used for microinjection of peptides. The cDNA for bovine leucine aminopeptidase was provided by Dr. A. Taylor (37). The stopcodon was replaced by a VSV tag, and the construct was cloned into pMT2. Isolated bLAP by anti-VSV antibodies was fully functional *in vitro*. Cos7 cells were transiently transfected with VSV-tagged LAP, fixed with methanol, and stained with anti-VSV antibodies and processed for confocal analysis 2 days after transfection. Endogenous TPPII was visualized by staining fixed Mel JuSo cells with the anti-TPPII antibody WL-26 (kindly provided by Martha Imreh, Karolinska Institute) before analysis by CLSM. For EM analysis, Mel JuSo cells were fixed in 0.5% glutaraldehyde and 4% paraformaldehyde in 0.1 M phosphate buffer (pH 7.2) and processed for ultrathin cryosectioning. Sections were incubated with purified mAb anti-human TAP1 198.3 (provided by R. Tampé, Germany) and analyzed by a Philips CM10 electron microscope (Eindhoven, The Netherlands).

### Synthetic Peptides

List of peptides used: fluorescent peptide, T[C-fluorescein]NKTERKY; quenched peptide, T[C-fluorescein]NKTER[K-Dabcyl]Y; FRET peptide, T[C-TetraMethylRhodamine]NRTER[C-fluorescein]Y; N-protected fluorescent peptide, Fmoc-T[C-fluorescein]NKTERKY; N-protected quenched peptide, Fmoc-T[C-fluorescein]NKTER[K-Dabcyl]Y; D-amino acid fluorescent peptide, TAE[K-fluorescein]TEKAY (all D-amino acids); p417, TVNKTERAY.

The photoreactive peptide 5PS1 (ERYNKSE-[BPA]-L) (22) and the various fluorescent peptides were synthesized using a Millipore 9050 Plus Pepsynthesiser. Fluorescein was covalently coupled to the cysteine residue using fluorescein-5-iodoacetamide (Molecular Probes, Leiden, The Netherlands). The photoreactive amino acid analog Fmoc BPA was obtained from Bachem AG (Bubendorf, Swiss). Fmoc-L-Lys(Dabcyl)-OH was obtained from Neosystems (France). The D amino acid fluorescent peptide was synthesized with an amidated

carboxyl terminus. All other peptides had a free COOH terminus. All peptides were HPLC purified (>95% pure) and further validated by mass spectrometry.

#### MHC Class I Stability

Cos7 cells were transiently transfected with VSV-bLAP in pMT2 or mock transfected with the empty pMT2 vector. Forty-eight hours after transfection, cells were cultured for 30 min in methionine/cysteine-free RPMI followed by labeling with 200  $\mu$ Ci  $^{35}$ S-methionine/cysteine for 1 hr. Cells were lysed in NP40-containing lysis mixture and split into equal halves. One half was incubated at 4°C and the other at 37°C for 30 min followed by immunoprecipitation with the mAb W6/32.

#### Peptide Translocation

Ten micrograms of the fluorescent peptide T[C-fluorescein]NKTERKY was radioiodinated with 400  $\mu$ Ci Na $^{125}$ I by chloroamine T catalyzed iodination. Peptide translocation was performed at 37°C with microsomes from human LCL cells in the presence or absence of 10 mM ATP for the times indicated. Translocated peptides were isolated by Con A-Sepharose (31).

#### Confocal Fluorescence Microscopy and FRAP Experiments

Confocal analysis of living cells was performed using a Leica TCS SP2 confocal system equipped with an Ar/Kr laser. For ATP depletion, cells were incubated for 30 min with a mixture of NaAz (0.05%) and 2-deoxyglucose (50  $\mu$ M) (14). For visualizing peptide binding to chromatin *in vitro*, peptides were mixed with isolated condensed frog sperm chromatin (provided by M. Fornerod, NKI) in PBS. Chromatin was decondensed by incubation with cytosolic extract. For FRAP analysis on chromatin *in vitro*, a part of one chromatin structure was bleached and fluorescence recovery was measured and compared with nearby (fluorescent peptide-bound) chromatin structures. For bleaching experiments to measure diffusion between the cytoplasm and the nucleus, a circular spot in the ER was bleached at full laser power, and an attenuated laser beam was used to monitor fluorescence levels in multiple regions (using Leica TCS time lapse). For line-scan FRAP analysis an external ArKr laser (25 mW) was coupled into the back focal plane of the objective via the epifluorescence excitation port, using a 30/70 beamsplitter, thus allowing simultaneous imaging and spot bleaching. Spots of 1.3  $\mu$ m (full width, half maximum) were bleached (>95%) using a single 30 ms pulse from the ArKr laser during data collection in line-scan mode at 1000 Hz. The half-time for recovery was calculated from each recovery curve after

correction for loss of fluorescence due to imaging (usually less than 4%). The diffusion coefficient D was determined as described (1). For peptide competition experiments *in vivo*, cells were incubated at 37°C in the presence of 10  $\mu$ M lactacystin for 60 min to inhibit proteasomes, coinjected with a 10-fold molar excess of nonfluorescent peptides, or incubated for 2 hr with influenza A virus strain A/NT/60/68 (1) before peptide injection. Mitotic cells were selected by their rounded-up appearance and aligned chromosomes, and analyzed by CLSM after microinjection of a mixture of N-terminally protected fluorescent peptides (ex/em: 488/520 nm) and EtBr (488/625 nm).

#### Chromatin Preparation, Peptide Crosslinking, and Mass Spectrometry

Chromatin was isolated using a modified protocol (38). Human sperm was washed twice with PBS at 4°C, followed by a single wash with HSP buffer (250 mM sucrose, 15 mM Tris-HCl [pH 7.4], 0.5 mM spermidine tetrachloride, and 0.2 mM spermine). Pelleted sperm was resuspended in 1 ml HSP including 0.3% n-octylglucoside and incubated for 5 min at room temperature. The remnants were washed twice with HSP buffer, aliquoted, and frozen until use. Peptide 5PS1 was iodinated with  $^{125}$ I by iodogen (Pierce)-catalyzed iodination. Chromatin was dissolved in 100  $\mu$ l PBS and incubated with 500 ng radio-iodinated 5PS1 in the absence or presence of ATP (1 mM) and competing peptide #417 for 2 min. This was followed by a single wash with PBS and 4 min exposure to UV light (UVP Blak-Ray B100A with Sylvania Par 38 mercury lamp) at a distance of 2 cm (22). Samples were washed twice with PBS before denaturation in sample buffer and analysis by SDS-PAGE. Coomassie-stained protein spots corresponding to the radiolabeled spots were excised after separation by 2D-IEF/SDS-PAGE. Following in-gel trypsin digestion, the resulting peptides were analyzed by HPLC and mass spectrometry (Q-ToF mass spectrometer, Micromass, Manchester, UK).

#### Peptide Degradation Analysis

Cells on coverslips were placed on an inverted Zeiss Axiovert 135 microscope equipped with a dry Achroplan 63x (NA 0.75) objective. Peptides were quantified by their red appearance (Dabcyl) using photospectrometry and mixed with Fura Red (Molecular Probes) as a microinjection marker. Excitation of both fluorescein and Fura Red was at 475 nm. A single cell was microinjected while simultaneously measuring fluorescence of a selected region containing the injected cell. Emission of fluorescein and Fura Red was measured after splitting the emitted light using a 580 nm dichroic mirror, and simultaneously detected with PTI model 612 analog photomultipliers.

## Immunity

For data acquisition, FELIX software (PTI Inc., USA) was used. For FRET analysis, fluorescein and TMR were excited at 475 or 545 nm. Emission of fluorescein and TMR was measured after splitting the emitted light using a 580 nm dichroic mirror with a 480–530 filter for fluorescein emission and a 590 filter for TMR emission, and simultaneously detected with PTI model 612 analog photomultipliers.

### Results

#### Distribution and Dynamics of Peptides in the MHC Class I Processing Pathway

To visualize different components of the MHC class I-processing pathway *in vivo*, the human melanoma cell line Mel JuSo was stably transfected with the proteasomal subunit LMP2 or the TAP subunit TAP1, both tagged with the green fluorescent protein (GFP) and analyzed by confocal microscopy (1, 14). Proteasomes were distributed over two compartments, the nucleus and the cytoplasm, and excluded from what is probably the ER, the nuclear envelope, and nucleoli (Figure 1A). The dynamics of GFP-tagged proteasomes were determined by bleaching a region in the cell and measuring subsequent recovery of fluorescence in the same region due to entry of surrounding fluorescent proteasomes. This technique is called fluorescence recovery after photobleaching (FRAP) (reviewed by (15–17)). FRAP showed that proteasomes freely diffuse within the nuclear and cytoplasmic compartment, and were only very slowly transported into the nucleus in a uni-directional manner (14). TAP1-GFP was localized to the ER network and the nuclear envelope (Figure 1A).

Previous studies showed that cytosolic peptides cannot be detected unless bound to MHC class I molecules (18) or small molecular weight proteins (5). This suggests that free peptides are unstable. To visualize peptide distribution *in vivo*, we generated a fluorescein-labeled peptide composed of D amino acids (TAE[K-fluorescein]TEKAY), which is protected from degradation by peptidases (data not shown). When microinjected in living cells, peptides distributed throughout the cytoplasm and the nucleus (Figure 1A). Since TAP does not recognize D peptides (19), the ER lumen was excluded. The peptide distribution resembled the distribution of proteasomes, but peptides were also present in nucleoli. A fraction of the peptides concentrated in the nucleus, suggesting interactions with nuclear factors. In order to determine the diffusion rate of peptides *in vivo*, a

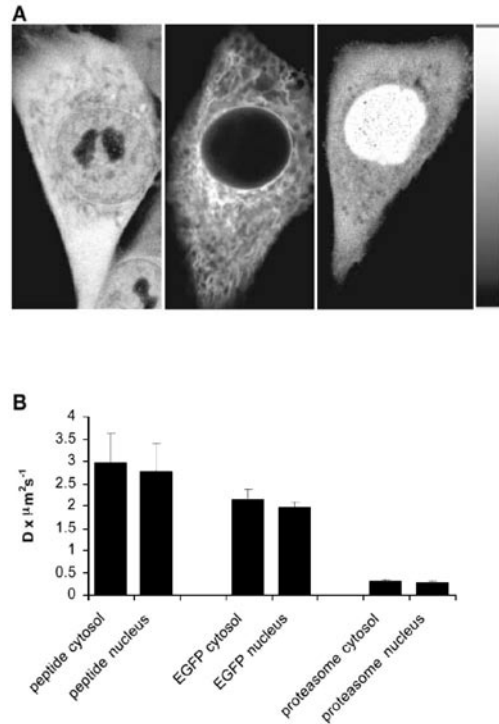


**Figure 1.** Distribution and Mobility of Proteasomes, TAP, and Peptides in Living Cells (A) The distribution of GFP-tagged proteasomes, GFP-tagged TAP, and fluorescein-labeled D peptides in living Mel JuSo cells at 37°C. Scalebar, 3  $\mu\text{m}$ . (B) Mobility of fluorescein-labeled D peptides, free GFP, and GFP-tagged proteasomes within the cytoplasm and the nucleus as determined by FRAP analysis measured in living Mel JuSo cells at 37°C.

line-scan FRAP protocol was applied (described in the **Experimental Procedures**). These experiments showed that peptides diffuse rapidly within the nuclear and cytoplasmic compartments. The mean mobility of free peptides was much faster than that of proteasomes (750 kDa for the 20S core) or free GFP (27 kDa) (Figure 1B). The mobility of peptides, GFP, and proteasomes was not affected by ATP depletion, implying that they move by diffusion (data not shown). A difference in diffusion of soluble proteins is mostly due to a difference in size, as reflected by the Stokes-Einstein formula that correlates the hydrodynamic behavior of a sphere mainly to its radius (20). Since fluorescent peptides moved faster than GFP, the majority of the introduced peptide molecules should be free rather than associated to larger diffusing proteins.

### Dynamics of Peptides in and between the Nucleus and the Cytoplasm

The high mobility of intracellular fluorescent peptides did not exclude that a fraction of these peptides was transiently associated to other structures. When these structures have a low mobility and a defined localization, associated peptides would behave accordingly. To visualize the dynamics of the different peptide fractions, a region in the cytoplasm or in the nucleus was bleached, and fluorescence was determined before and after bleaching for both compartments. When a cytoplasmic region was bleached, fluorescence recovered to levels comparable to other cytoplasmic regions within the same cell (Figure 2A, cytoplasm region 1 was bleached). Nuclear fluorescence also decreased but remained higher compared to the cytoplasm. Apparently, peptides can freely diffuse through the cytoplasm and between the cytoplasmic and the nuclear compartment.

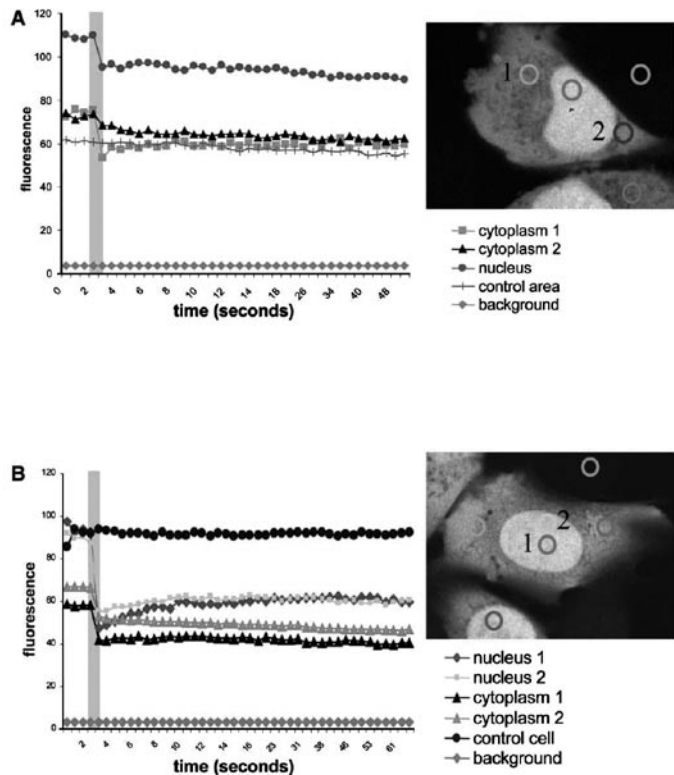
To measure the mobility of the nuclear peptide fraction, a region in the nucleus was bleached. A decrease in both cytoplasmic and nuclear fluorescence was ob-

served due to rapid diffusion rate of the mobile pool of peptides (Figure 2B, nucleus region 1 was bleached). When compared to the cytoplasm, fluorescent recovery within the bleached area of the nucleus was slower, suggesting that a fraction of the microinjected peptide pool is interacting with nuclear molecules. Apparently nuclear peptides are present in two pools, a mobile fraction in rapid equilibrium with the cytoplasm, and a relatively slower pool bound to nuclear proteins. ATP depletion did not affect the rate of peptide mobility or the accumulation in the nucleus (data not shown), suggesting that peptides move by diffusion and that nuclear accumulation is not the result of an active (ATP-dependent) process.

### Peptides Bind to Chromatin-Associated Proteins

The immobile nuclear peptide pool appeared to be equally distributed throughout the nucleus and was not enriched in areas like nuclear speckles. Possible peptide binding proteins within the nucleus are chromatin-associated proteins, as the chromatin network is widely distributed and relative immobile (21). To examine whether chromatin has a peptide binding

**Figure 2.** Dynamics of Peptides in and between Nucleus and Cytoplasm (A) Dynamics of cytoplasmic fluorescent D peptides in living Mel JuSo cells at 37°C. After introduction of peptides by microinjection, fluorescence in cytoplasmic region 1 was bleached, and fluorescence was monitored in the indicated cytoplasmic and nuclear regions. The graph quantifies levels of fluorescence within the indicated regions before and after bleaching. The gray bar indicates the bleaching. (B) Dynamics of nuclear fluorescent D peptides. After introduction of the peptide by microinjection, region 1 in the nucleus was bleached, and fluorescence was monitored in the indicated nuclear and cytoplasmic regions. The graph quantifies levels of fluorescence within the indicated regions before and after bleaching. The gray bar indicates the bleaching.



## Immunity

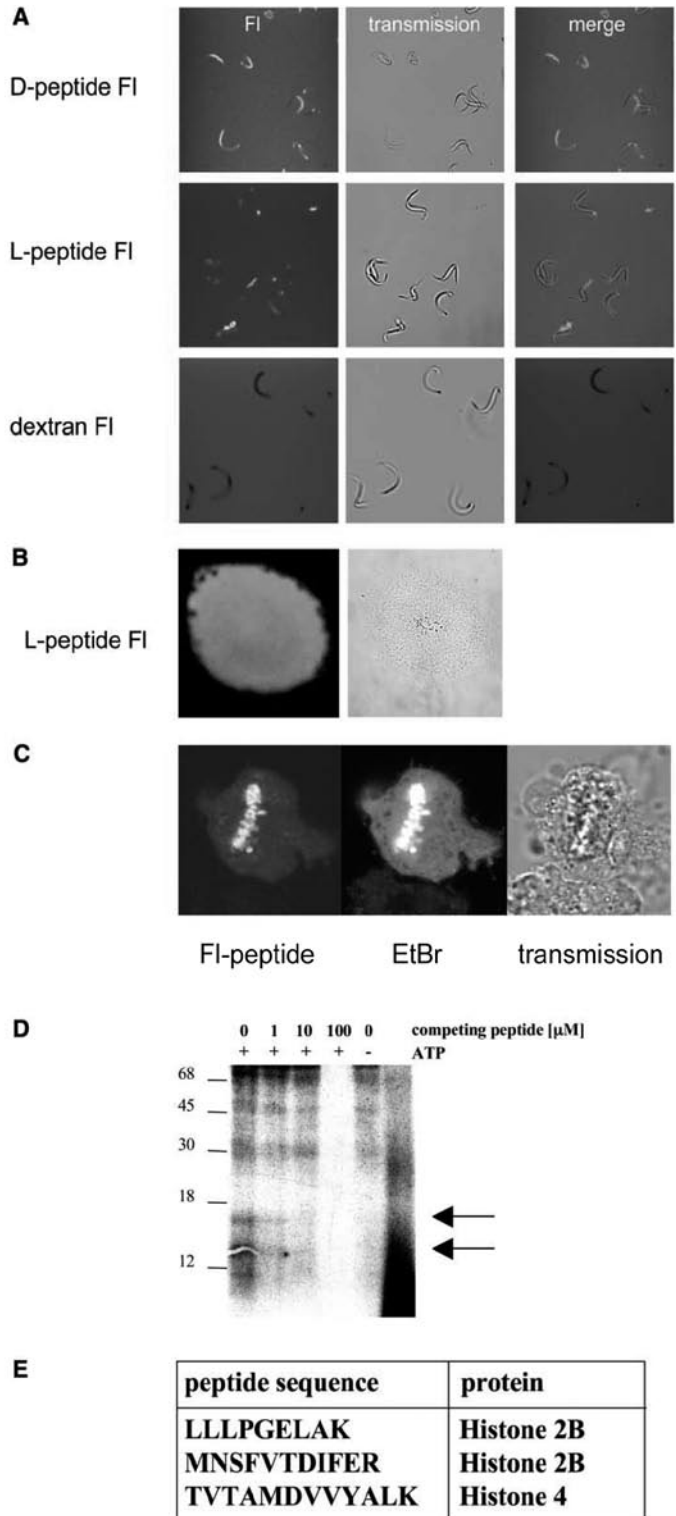
**Figure 3.** Binding of Peptides to Chromatin-Associated Molecules.

**(A)** Binding of peptides to chromatin *in vitro*. Fluorescein-labeled D peptide (top panel), L peptide (middle panel), or dextran (bottom panel) was added to purified frog sperm chromatin, and distribution was visualized by confocal imaging.

**(B)** Binding of peptides to decondensed chromatin *in vitro*. Fluorescent L peptides were added to purified frog sperm chromatin decondensed *in vitro*, and distribution was visualized by confocal imaging. **(C)** Peptide distribution during mitosis. N-terminally protected fluorescent L peptide Fmoc[C-fluorescein]NKTERKY was coinjected with ethidium bromide (EtBr, to stain DNA) into mitotic Mel JuSo cells and analyzed by CLSM. The transmission image shows aligned and condensed chromosomes that stain for the fluorescent peptides and EtBr, as indicated.

**(D)** Identification of peptide binding nuclear proteins. Purified human chromatin was incubated with radio-iodinated peptide 5PS1 in the presence or absence of ATP or competing peptide p417. After UV exposure, chromatin was analyzed by 15% SDS-PAGE. A limited set of radiolabeled proteins was visualized. Arrows indicate the two proteins identified. The last lane represents the iodinated peptide 5PS1.

**(E)** Peptide binding chromatin-associated proteins. Human chromatin-associated proteins were separated by 2D IEF/SDS-PAGE, and spots corresponding to photoaffinity-labeled proteins were excised. Peptide fragments were analyzed by mass spectrometry. The peptide sequence and corresponding proteins are indicated.



capacity, isolated condensed frog sperm chromatin was incubated with the fluorescein-labeled L and D amino acid peptides *in vitro*. Fluorescent peptides accumulated on condensed chromatin (Figure 3A, top two panels). To exclude that binding is fluorescein-mediated, fluorescein-labeled dextran was incubated with chromatin. A negative image was observed, indicating that dextran-fluorescein was excluded from chromatin (Figure 3A, bottom panel). To further exclude an effect of the packing of condensed chromatin, decondensed frog chromatin was generated *in vitro*, which formed an artificial nucleus. Similar to condensed chromatin, fluorescent L peptides accumulated on decondensed chromatin (Figure 3B). FRAP experiments on both forms of chromatin incubated with fluorescent peptides showed recovery of fluorescence in the bleached area (data not shown), suggesting dynamic chromatin association.

One exception to the cytoplasm/nucleus two-compartment peptide model is mitosis when the nuclear envelope is dissolved, and cytoplasmic peptidases and peptide binding chromatin are not physically separated. To test whether fluorescent peptides still associate to chromatin during mitosis, the N-terminally protected fluorescent L peptide was coinjected with ethidium bromide (to stain DNA) into mitotic Mel JuSo cells. Fluorescent peptides associated very efficiently with the aligned condensed chromosomes during mitosis (Figure 3C). This may provide protection against cytosolic peptidases which are no longer separated from chromosomes by the nuclear envelope.

To determine which nuclear proteins were able to bind peptides, a photoaffinity-labeling experiment was performed with the radio-iodinated peptide 5PS1 (22). This peptide contained a photoreactive group that allowed covalent photoaffinity labeling upon UV exposure. Isolated condensed human sperm chromatin was briefly incubated with peptide 5PS1 in the absence or presence of ATP and competing nonradioactive peptides, and subsequently exposed to UV light. A number of proteins were visualized in the absence or presence of ATP (Figure 3D). Incubation with increasing amounts of competing, cold peptides resulted in a concentration-dependent decrease of photoaffinity-labeled proteins. To identify the peptide binding proteins, these proteins were separated by 2D IEF/SDS-PAGE. In a parallel experiment nonlabeled proteins were separated and stained by Coomassie, and spots corresponding to the photoaffinity-labeled proteins were analyzed by mass spectrometry after

trypsin digestion. Peptides were sequenced (Figure 3E) and identified as histone H2B and H4.

#### Peptides and TAP Location

The TAP transporter is present in the ER membrane and the connected nuclear envelope (Figure 4A). The outer nuclear membrane is directly connected to the ER membrane, while the inner membrane facing the nucleoplasm is connected with the outer membrane via the pore membrane domain, which restricts diffusion of large transmembrane molecules (23, 24). Nuclear peptides could either enter the cytoplasm to reach TAP present in the ER membrane or directly access TAP from the nuclear side of the nuclear envelope. If so, peptides would be entering the ER lumen from two different compartments: the cytoplasm, containing peptidases like TPPII and LAP (Figure 5B), and the nucleus. To determine whether TAP was present in the inner nuclear membrane, we repeatedly bleached TAP-GFP-expressing cells to deplete the fluorescent pool of TAP molecules within the ER region. Repeated bleaching of a membrane region will ultimately lead to loss of fluorescence of molecules diffusing within connected membranes (25), a variation of FRAP called FLIP (fluorescence loss in photobleaching) (26). Since the nuclear pore restricts diffusion, only TAP present in the outer nuclear membrane can rapidly be exchanged with TAP present in the ER network. Three regions in the ER network were bleached, each for a period of 10 s, resulting in an almost complete loss of fluorescence of the ER network. When measuring fluorescence of the nuclear envelope, fluorescence dropped to the same level with almost identical dynamics (Figure 4A). If TAP had been equally distributed over the inner and outer membranes of the nuclear envelope, a reduction in fluorescence of about 50% would have been observed. However, a loss of around  $93 \pm 3\%$  (mean  $\pm$  SEM,  $N = 6$ ) of fluorescent TAP-GFP in the nuclear envelope was observed. Apparently, the nuclear envelope was able to exchange virtually all TAP transporters with the pool of TAP transporters bleached in the ER network.

To confirm that TAP is distributed only on the cytoplasmic face of the nuclear envelope, untransfected Mel JuSo cells were fixed and cryosections were stained with antibodies against the cytoplasmic nucleotide binding domain of TAP1. Electron microscopy showed gold particle staining exclusively on the cytoplasmic side of the nuclear envelope (Figure 4B, 150

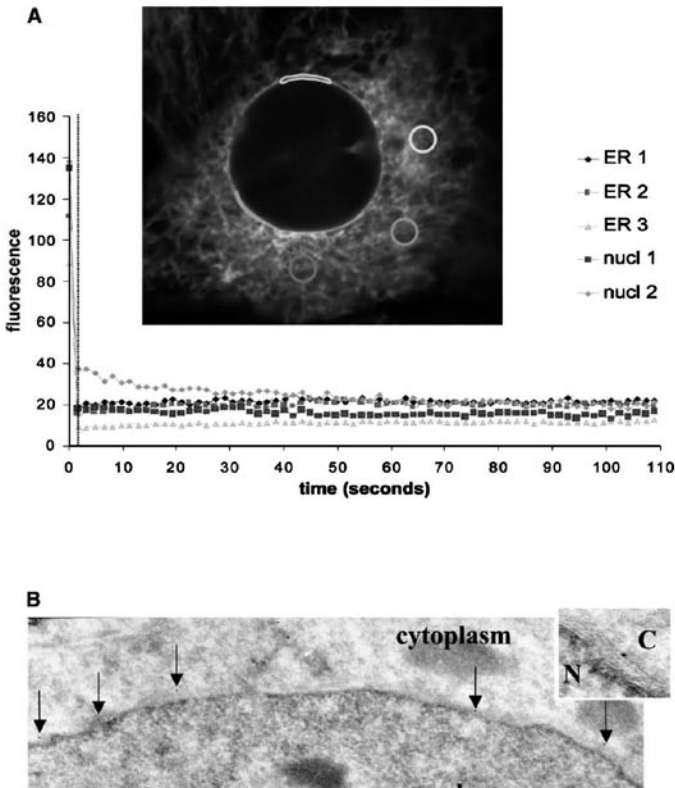


**Figure 4.** TAP in the Nuclear Envelope (A) Living Mel JuSo cells expressing TAP-GFP were analyzed at 37°C.

Different regions in the ER network (indicated by ER1-3) were bleached, and loss in fluorescence was measured as a function of time in the bleached ER regions and in two indicated regions in the nuclear envelope (nucl 1 and 2) of the same cell. The quantitation shows similar loss in fluorescence of the nuclear envelope and the ER network. The slight delay in the second nuclear region is probably due to its distance from the bleached ER regions. (B) Mel JuSo cells were fixed, and cryosections were labeled with an antibody against the nucleotide binding domain of TAP1 followed by immunogold (10 nm) labeling. Arrows show the location of gold particles close to the nuclear envelope. The inset shows a higher magnification of the double membrane of the nuclear envelope. The cytoplasm (C) and nucleus (N) are indicated. Magnification, 11,500 $\times$  (inset 46,000 $\times$ ).

gold particles on the cytoplasmic side, none on the nuclear side). TAP is apparently excluded from the nuclear face of the nuclear envelope in agreement with the data obtained from FLIP analysis. These findings imply that nuclear peptides have to enter the cytoplasm for TAP translocation into the ER lumen.

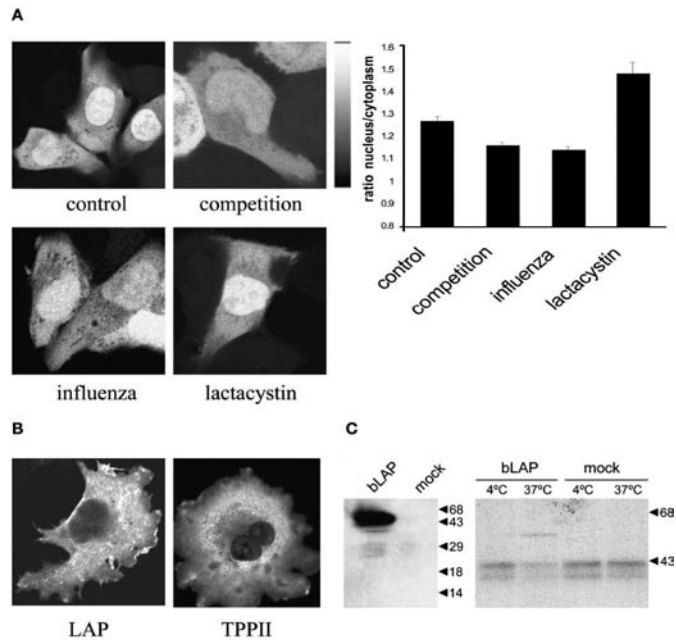
#### Endogenous Peptides in Living Cells

In our study, fluorescent peptides were introduced in cells to describe the dynamics of peptides *in vivo*. To test whether the fluorescent peptides do behave like endogenous peptides, we examined competition of fluorescent peptides with endogenous peptides for nuclear accumulation. Therefore an N-terminally modified fluorescent L peptide (Fmoc-T[C-fluorescein]NKTERKY) was used that was protected against aminopeptidases (shown later). These peptides showed an intracellular distribution similar to that of D peptides (Figure 5A). First, fluorescent peptides were microinjected in the presence of a 10-fold molar excess of its nonfluorescent counterpart (Figure 5A). Accumulation of fluorescence decreased

in the nucleus (a fluorescence nucleus/cytoplasm ratio of 1.16 instead of 1.27 when injected with fluorescent peptides only), implying that peptides competed for nuclear binding. To increase the pool of endogenous peptides, cells were infected with influenza virus (1). Again, fluorescent peptide accumulation within the nucleus dropped (to a ratio of 1.14), implying that microinjected peptides competed with endogenous peptides for nuclear binding. To decrease competition for nuclear binding, cells were incubated with the proteasome inhibitor lactacystin for 1 hr to deplete the endogenous peptide pool. Nuclear accumulation of introduced fluorescent peptides increased (ratio of 1.48), suggesting that more peptide binding sites were available. Apparently endogenous peptides behaved similarly to fluorescent peptides and actually competed with each other for nuclear binding. The amount of introduced fluorescent peptides (approximately  $2 \times 10^5$  peptides) should be comparable to the endogenous pool since nuclear binding of fluorescent peptides can be reduced by increasing and improved by eliminating the endogenous peptide pool.

**Figure 5.** Endogenous Peptides in Living Cells **(A)** Fluorescent peptides compete with endogenous peptides for binding to nuclear proteins. The ratio of nuclear versus cytoplasmic fluorescence was determined. Cells were injected with an N-terminally protected fluorescent L peptide, either alone or with competing (nonfluorescent) peptides. Competition with endogenous peptides for nuclear binding was tested by infecting cells with influenza virus (increasing the endogenous peptide pool) or treatment with lactacystin (blocking the proteasome) (mean  $\pm$  SEM, N = 9).

**(B)** The intracellular distribution of two peptidases. Tagged bovine LAP was transiently expressed in Cos7 cells. Endogenous TPPII was examined in Mel JuSo cells. Cells were fixed, stained with antibodies, and analyzed by CLSM. **(C)** Overexpressing bLAP reduces the peptide pool for MHC class I loading. Western blot analysis of lysates generated from Cos7 cells after transfection with VSV-bLAP (left panel). The same Cos7 cells were biosynthetically labeled with  $^{35}\text{S}$ -Met/Cys for 1 hr. Lysates were incubated at either 4°C or 37°C for 30 min before isolation of MHC class I complexes and separated by 10% SDS-PAGE.



Still, the pool of peptides presented by MHC class I may not be diffusing freely through the cell but may instead be protected against degradation by binding to and transfer by chaperones, or directly delivered to TAP by proteasomes. To test this, VSV-tagged bovine leucine amino peptidase (bLAP) was overexpressed in Cos7 cells. VSV-tagged bLAP was present in the cytoplasm but excluded from the nucleus (**Figure 5B**). This was identical to the distribution of the peptidase TPPII in Mel JuSo cells, which was also excluded from the nucleus (**Figure 5B**). Western blotting of VSV-bLAP transfected Cos7 cells revealed bLAP in transfected cells (**Figure 5C**, left panel). Forty-eight hours after transfection, VSV-bLAP and mock-transfected cells were biosynthetically labeled for 1 hr. NP40 lysates were split in halves and either maintained at 4°C (to stabilize both peptide-loaded and free MHC class I molecules) or 37°C (to dissociate the peptide-free MHC class I molecules) for 30 min before isolation of stable MHC class I complexes with the mAb W6/32

(27). Whereas MHC class I molecules were temperature stable (i.e., peptide-loaded) in mock-transfected cells, about half of the MHC class I molecules dissociated under these conditions in cells overexpressing bLAP (**Figure 5C**). Apparently, an increase in peptidase activity reduces the available peptide pool for MHC class I molecules. These peptides should be free to access the active center of peptidases like bLAP (28) which suggests that a large pool of peptides destined for MHC class I loading can also be substrate for cytosolic peptidases.

#### Peptide Degradation in Living Cells

To detect peptidase activity *in vivo*, we designed a 9-mer L amino acid peptide that would become fluorescent only after degradation by peptidases. The quenched peptide (T[C-fluorescein]NKTER[K-Dabcyl]Y) contains a fluorescein group and a Dabcyl quencher group coupled to amino acids 2 and 8, respectively. The Dabcyl group efficiently quenches emission of the nearby fluorescein group, and fluorescence will only be detected when amino acids 2 and 8 are separated as the result of peptidase activity (**Figure 6A**). When added to PBS *in vitro*, fluorescence remained very low (**Figure 6B**,  $t = 0$ ). However, when a cytosolic extract containing peptidases was added (arrow), fluorescence rapidly increased due to separation

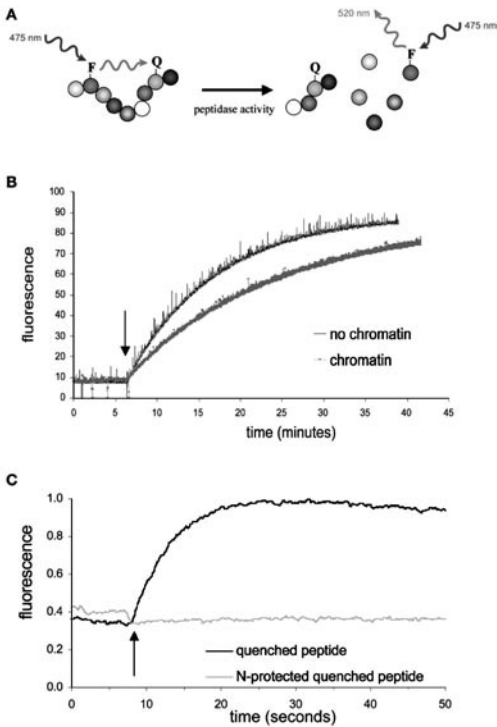


**Figure 6.** Peptide Degradation in Living Cells

(A) Detecting peptidase activity. The quenched-fluorescent peptide T[C-fluorescein]NKTER[K-Dabcyl]Y contains a fluorescein group (F) and a Dabcyl quencher group (Q). The quencher Q efficiently absorbs emission of the nearby fluorescein group F, and fluorescence will only be detected when these amino acids are separated following peptidase activity.

(B) Degradation of peptides *in vitro*. Quenched-fluorescent peptides were incubated in PBS in the absence or presence of purified frog sperm chromatin. Only when cytosol was added (arrow), degradation of peptides was observed by an increase in fluorescence. The presence of chromatin reduced the rate of degradation. (C) Degradation of quenched fluorescent peptide and its N-terminally protected form in living Mel JuSo cells at 37°C. At the time point indicated (arrow), equal amounts of either unprotected or N-terminally protected quenched-fluorescent peptides were microinjected.

of the quencher and the fluorescein moiety. Since binding to chromatin may temporarily protect peptides against degradation, we did the same experiment in the presence of purified chromatin. Upon addition of cytosol, a reduced rate of peptide degradation was observed (Figure 6B) due to the dynamic interaction between peptides and chromatin.

The peptide degradation experiment was repeated *in vivo* by microinjecting the quenched peptide into Mel JuSo cells. Fluorescence appeared almost immediately after microinjection (Figure 6C, indicated by arrow). Degradation went to completion with a half-life of 7 s ( $t_{1/2} = 7.0 \pm 1.1$  s, mean  $\pm$  SD). Prolonged measurement of microinjected cells (up to 5–10 min) did not show any further increase in fluorescence. The process of degradation was not saturated because microinjection of a 10-fold higher amount of this peptide yielded identical degradation rates (data not shown). To exclude any effect on the quencher molecule, resulting in increased fluorescence without degradation of the peptide, the same experiments were repeated with a 9-mer peptide containing a fluorescein and a tetramethylrhodamine (TMR) FRET pair (T[C-TMR]NRTER[C-fluorescein]Y). Microinjection of this peptide resulted in decreased red and increased green fluorescence when the fluorescein was excited (at 475 nm), indicating separation of the two fluorophores. No change in red (TMR) fluorescence was measured when the TMR was excited directly (at 545 nm) (data not shown). Apparently, the acceptor group was not quenched after microinjection in living cells.

It is unclear whether small peptides are targeted exclusively by aminopeptidases or also by carboxy and endopeptidases (including the proteasome) *in vivo*. Aminopeptidase activity can be inhibited by modifying the free N terminus of the peptide (4). We repeated the experiment as described above and microinjected the same quenched-fluorescent peptide coupled to an N-terminal Fmoc group (Fmoc-T[C-fluorescein]NKTER[K-Dabcyl]Y). No increase in fluorescence was observed, implying that this peptide was not degraded (Figure 6C) and that the quencher was not inactivated. This suggests that *in vivo* aminopeptidases are responsible for the degradation of these peptides, instead of carboxy and endopeptidases (like the proteasome).

Since introduced peptides have to compete with endogenous peptides for degradation or potential binding to chaperones, we treated cells with lactacystin to block peptide generation by the proteasome resulting in a small increase in the half-life ( $t_{1/2} = 9.7 \pm 1.3$  s, mean  $\pm$  SD). Cells were also treated with cycloheximide to inhibit protein synthesis. This resulted in less endogenous peptides generated from newly synthesized proteins (1) and should enhance the pool of peptide-receptive chaperones normally involved in protein folding. Again, only a small increase in

the half-life of microinjected peptides was observed ( $t_{1/2} = 8.7 \pm 1.4$  s). ATP depletion did not affect the half-life. Together these data suggest that most introduced peptides are not protected but rapidly degraded by cytosolic peptidases.

#### Peptide Degradation versus TAP Translocation

Fluorescent N-protected L peptides rapidly moved in the cytoplasm (faster than a 27 kDa protein GFP, **Figure 1B**) and were not excluded by the nuclear pore, indicating that they were not associated with proteins larger than 50–60 kDa (29), including most heat shock proteins. Although they can associate to HSPs *in vitro* (30), these peptides were not translocated into the ER because peptides require a free N terminus for recognition by TAP (31). To examine the relative efficiencies of peptide degradation versus translocation into the ER (mimicking the *in vivo* situation), we introduced a fluorescein-labeled peptide (T[C-fluorescein]NKTERKY). This unprotected fluorescent peptide contained an N-linked glycosylation site that would be glycosylated and retained in the ER when translocated by TAP (31). To show translocation of this peptide into the ER, the peptide was iodinated and incubated for various times with human microsomes in the absence or presence of ATP. Glycosylated peptides were recovered by Con A-Sepharose and quantified (**Figure 7A**). The iodinated fluorescent peptide was translocated by TAP in a time- and ATP-dependent fashion.

If a substantial fraction of introduced peptides would be translocated by TAP, the ER lumen would accumulate fluorescence. To compare the rate of peptidase activity versus peptide translocation by TAP *in vivo*, the fluorescent peptide was microinjected into Mel JuSo cells and cultured for 30 min. Confocal analysis showed a random distribution in the nuclear and cytoplasmic compartment, and some exclusion from the ER region (**Figure 7B**). This represented the distribution of a peptide degradation product that differed from the distribution of an N-terminally protected peptide that was not degraded. If translocation by TAP would be as efficient as peptide degradation *in vivo*, a substantial fraction of the fluorescent peptide pool would accumulate in the ER despite the short half-life of similar 9-mer peptides. Once translocated into the ER by TAP, the fluorescent peptide is glycosylated and can be distinguished from cytosolic peptides and peptide degradation products by bleaching the nuclear peptide pool. Since peptides diffused freely between the nu-

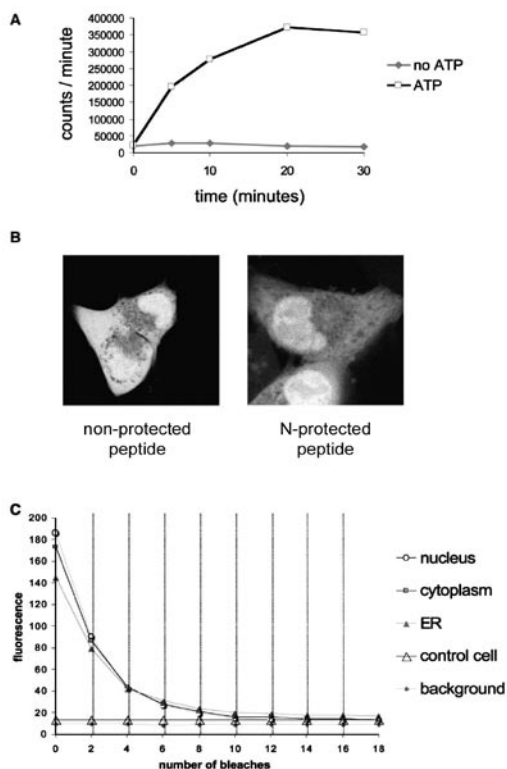


**Figure 7.** Peptide Degradation and TAP Translocation in Living Cells (A) Fluorescent peptides are translocated by TAP. Iodinated peptide T[C-fluorescein]NKTERKY was incubated with microsomes at 37°C in the presence or absence of ATP for the times indicated. Translocated peptides were isolated and quantified. (B) Distribution of free and N-terminal protected fluorescent peptides (T-C[fluorescein]NKTERKY) upon microinjection in living Mel JuSo cells. (C) Peptide degradation versus TAP-translocation *in vivo*. The fluorescent peptide T[C-fluorescein]NKTERKY was microinjected in Mel JuSo cells and analyzed after 30 min. The peptide contains a glycosylation site retaining it in the ER after translocation by TAP. Using a fluorescence loss in photobleaching protocol, fluorescent nuclear and cytosolic peptides were depleted by repeatedly bleaching a nuclear region within one cell for 2 s with intervals allowing redistribution of diffusing peptides (bleaches indicated by the dashed lines). Fluorescence in the nucleus, cytoplasm, ER, and a control cell are quantified.

cleus and cytoplasm, the cytosolic pool of free fluorescent peptides would decrease as well (see also **Figure 2B**). To deplete the cell of cytosolic fluorescence without affecting translocated peptides within the ER lumen, the nucleus was bleached multiple times and the effects on cytoplasmic and ER fluorescence were

## Immunity

quantified. Repeated bleach pulses quantitatively reduced both nuclear and cytosolic fluorescence close to background levels (Figure 7C). Apparently, no substantial pool of (glycosylated) fluorescent peptides was retained in the ER lumen, suggesting that peptide degradation was far more efficient than peptide translocation into the ER by TAP.

### Discussion

The MHC class I antigen presentation pathway is a dynamic process involving protein degradation and presentation of the resulting peptides. Various dedicated proteins are involved in this pathway, including the peptide transporter TAP, a specialized chaperone tapasin and immuno-proteasomal subunits. Still, both theoretical calculations and experimental data suggest that antigen processing is very inefficient. It has been estimated that on average  $10^2$  (32) to  $10^4$  (9, 10) proteins need to be degraded for every single peptide in a MHC class I complex. Since the processes of peptide transport by TAP (1) and peptide binding by MHC class I molecules (33) are not occurring at saturated levels, many peptides are possibly lost between generation by the proteasome and association with TAP. Only little is known about the fate of these peptides, which is surprising as it is an important phase in the sequence of events resulting in antigen presentation.

Here we have studied the fate of peptides in living cells. Like proteasomes, peptides are located in both the cytoplasmic and nuclear compartments, but unlike proteasomes (14) peptides rapidly diffuse into and out of the nucleus. The nuclear pore connecting these two compartments does not form a diffusion barrier for small particles like peptides. Still, these compartments are different from the peptide's point of view. First, certain peptidases like TPP1 and LAP are excluded from the nuclear compartment. Such large peptidase complexes would require a nuclear localization signal to enter the nucleus. It is unknown whether the nucleus contains peptidases at all, as chromatin lacks such activities. There is, however, no explicit need for nuclear peptidases since peptides generated in the nucleus can rapidly enter the cytoplasm. Second, the dynamic interaction of peptides with chromatin reduces their availability as substrates for peptidases. Interacting proteins include histone H2B and histone H4. It is unclear why these histones have some affinity for peptides. Since histones are expressed at high levels, accumulation of peptides in the nucleus may be the result. Shastri and coworkers identified

a peptide pool associated to small molecular weight proteins (around 20 kDa) (5) that could represent histones (14 kDa). It remains to be examined whether chromatin influences delivery of a specific peptide pool to the MHC class I presentation pathway and whether peptides bind with different affinities. The binding of peptides to chromosomes may temporarily protect peptides derived from short-lived proteins specifically expressed during mitosis, until the ER has been reassembled after cell division and production of MHC class I molecules is restored. The observation that peptides bind to chromatin could be relevant for vaccination and crosspriming with apoptotic bodies. By preventing accessibility to peptidases, chromatin could stabilize peptides during apoptosis or necrosis and would thereby improve successful peptide delivery to antigen-presenting cells (APCs) in a similar way as suggested for gp96 and other chaperones.

We showed that peptides are degraded *in vivo* by amino-peptidases. No carboxypeptidase activity was detected. Proteasomes have been reported to generate the correct C-terminus of presented peptides but not necessarily the correct N-terminus (34). Aminopeptidases can further trim the peptide to the correct size for MHC class I binding and beyond. Correct generation of the peptide C-terminus is essential when carboxypeptidase activity is absent, underlining the need for correct C-terminal cleavage by the proteasome, especially when ER peptidases lack carboxypeptidase activity for such trimming (5, 6, 35).

While most peptides simply diffuse from proteasomes to TAP, it cannot be excluded that some proteasomes directly deliver their peptides to TAP. However, a direct association between proteasomes and TAP has never been found. Moreover, since TAP is absent in the nucleus, direct delivery of peptides derived from nuclear proteins would be impossible. By overexpressing the peptidase LAP, a clear reduction in peptide loading of MHC class I molecules is observed. Not all peptides for MHC class I molecules were destroyed which could be due to LAP specificity or simply because some peptides contact TAP before peptidases. Still, these data indicate that a large fraction of peptides destined for MHC class I loading are targeted by cytosolic peptidases. This peptide pool must be free to access peptidases and are not protected by chaperones or directly delivered by proteasomes to TAP. We cannot, however, exclude that a fraction of peptides is not freely diffusing and is not handled differently. Still, the majority of peptides is free rather than associated

to cytosolic chaperones. This is evident from various observations including FRAP data showing free mobility of peptides in the cytoplasm and unhindered transfer through the nuclear pore. Furthermore, all introduced peptides are rapidly degraded even when the available chaperone pool is increased. This suggests that *in vivo* peptide-chaperone interactions are at best very transient if occurring at all. Still, highly efficient delivery of gp96 or other ER chaperone-associated peptides into the MHC class I pathway has been reported (13, 36). This can be envisioned when such a protein-peptide complex is relatively stable and able to deliver peptides efficiently to the MHC class I-loading complex. This may also be the case for chromatin-bound peptides during uptake of apoptotic bodies.

We have shown by confocal imaging and electron microscopy that TAP is excluded from the nuclear side of the nuclear envelope. This implies that nuclear peptides have to leave the nucleus through the nuclear pore and enter the cytoplasmic compartment before they can encounter TAP. Given their rate of diffusion (around  $3 \mu\text{m}^2\text{s}^{-1}$ ), a peptide will move about  $2.45 \mu\text{m}$  per s (calculated with Einstein's for-

mula  $x^2 = 2Dt$ , with  $x^2$ , average value for the square of the distance; D, diffusion coefficient; and t, time). A peptide will thus diffuse through the entire cell in 6 s and has to find TAP within this short period for translocation into the ER lumen. Nine-mer peptides have a very short half-life *in vivo* (around 7 s), and given the number of TAP molecules expressed in a cell (and the time required for translocation), the chance of making the correct interaction is very small. This is further illustrated by the observation that introduction of a fluorescent peptide with a glycosylation site in living cells showed no accumulation in the ER where the translocated peptide would have been retained. Apparently, cytoplasmic peptide degradation is far more efficient than peptide translocation into the ER lumen.

### Acknowledgements

We would like to thank Carla Herberts, Helen Pickersgill, and Maarten Fornerod for critical reading and helpful suggestions, and Willemien Benckhuijsen and Henk Hilkmann for peptide synthesis and purification. This work was supported by grants from NWO (Pionier) and the Dutch Cancer Society.

### References

1. Reits, E.A., et al., The major substrates for TAP *in vivo* are derived from newly synthesized proteins. *Nature*, 2000. 404(6779): p. 774-778.
2. Schubert, U., et al., Rapid degradation of a large fraction of newly synthesized proteins by proteasomes. *Nature*, 2000. 404(6779): p. 770-774.
3. Rock, K.L., et al., Inhibitors of the proteasome block the degradation of most cell proteins and the generation of peptides presented on MHC class I molecules. *Cell*, 1994. 78(5): p. 761-771.
4. Mo, X.Y., et al., Distinct proteolytic processes generate the C and N termini of MHC class I-binding peptides. *J Immunol*, 1999. 163(11): p. 5851-5859.
5. Paz, P., et al., Discrete proteolytic intermediates in the MHC class I antigen processing pathway and MHC I-dependent peptide trimming in the ER. *Immunity*, 1999. 11(2): p. 241-251.
6. Serwold, T., et al., ERAAP customizes peptides for MHC class I molecules in the endoplasmic reticulum. *Nature*, 2002. 419(6906): p. 480-483.
7. Koopmann, J.O., et al., Export of antigenic peptides from the endoplasmic reticulum intersects with retrograde protein translocation through the Sec61p channel. *Immunity*, 2000. 13(1): p. 117-127.
8. Roelse, J., et al., Trimming of TAP-translocated peptides in the endoplasmic reticulum and in the cytosol during recycling. *J Exp Med*, 1994. 180(5): p. 1591-1597.
9. Montoya, M. and M. Del Val, Intracellular rate-limiting steps in MHC class I antigen processing. *J Immunol*, 1999. 163(4): p. 1914-1922.
10. Yewdell, J.W., Not such a dismal science: the economics of protein synthesis, folding, degradation and antigen processing. *Trends Cell Biol*, 2001. 11(7): p. 294-297.
11. Geier, E., et al., A giant protease with potential to substitute for some functions of the proteasome. *Science*, 1999. 283(5404): p. 978-981.
12. Beninga, J., K.L. Rock, and A.L. Goldberg, Interferon-gamma can stimulate post-proteasomal trimming of the N terminus of an antigenic peptide by inducing leucine aminopeptidase. *J Biol Chem*, 1998. 273(30): p. 18734-18742.
13. Binder, R.J., N.E. Blachere, and P.K. Srivastava, Heat shock protein-chaperoned peptides but not free peptides introduced into the cytosol are presented efficiently by major histocompatibility complex I molecules. *J Biol Chem*, 2001. 276(20): p. 17163-17171.
14. Reits, E.A., et al., Dynamics of proteasome distribution in living

- cells. *Embo J*, 1997. 16(20): p. 6087-94.
15. Lippincott-Schwartz, J., E. Snapp, and A. Kenworthy, Studying protein dynamics in living cells. *Nat Rev Mol Cell Biol*, 2001. 2(6): p. 444-456.
  16. Meyvis, T.K., et al., Fluorescence recovery after photobleaching: a versatile tool for mobility and interaction measurements in pharmaceutical research. *Pharm Res*, 1999. 16(8): p. 1153-62.
  17. Reits, E.A. and J.J. Neeffjes, From fixed to FRAP: measuring protein mobility and activity in living cells. *Nat Cell Biol*, 2001. 3(6): p. 145-147.
  18. Falk, K., et al., Allele-specific motifs revealed by sequencing of self-peptides eluted from MHC molecules. *Nature*, 1991. 351(6324): p. 290-296.
  19. Gromme, M., et al., The rational design of TAP inhibitors using peptide substrate modifications and peptidomimetics. *Eur J Immunol*, 1997. 27(4): p. 898-904.
  20. Arrio-Dupont, M., et al., Mobility of creatine phosphokinase and beta-enolase in cultured muscle cells. *Biophys J*, 1997. 73(5): p. 2667-2673.
  21. Phair, R.D. and T. Misteli, High mobility of proteins in the mammalian cell nucleus. *Nature*, 2000. 404(6778): p. 604-609.
  22. Spee, P., J. Subjeck, and J. Neeffjes, Identification of novel peptide binding proteins in the endoplasmic reticulum: ERp72, calnexin, and grp170. *Biochemistry*, 1999. 38(32): p. 10559-10566.
  23. Ellenberg, J., et al., Nuclear membrane dynamics and reassembly in living cells: targeting of an inner nuclear membrane protein in interphase and mitosis. *J Cell Biol*, 1997. 138(6): p. 1193-1206.
  24. Soullam, B. and H.J. Worman, Signals and structural features involved in integral membrane protein targeting to the inner nuclear membrane. *J Cell Biol*, 1995. 130(1): p. 15-27.
  25. Poo, M. and R.A. Cone, Lateral diffusion of rhodopsin in the photoreceptor membrane. *Nature*, 1974. 247(441): p. 438-441.
  26. Cole, N.B., et al., Diffusional mobility of Golgi proteins in membranes of living cells. *Science*, 1996. 273(5276): p. 797-801.
  27. Schumacher, T.N., et al., Direct binding of peptide to empty MHC class I molecules on intact cells and in vitro. *Cell*, 1990. 62(3): p. 563-567.
  28. Burley, S.K., et al., Structure determination and refinement of bovine lens leucine aminopeptidase and its complex with bestatin. *J Mol Biol*, 1992. 224(1): p. 113-140.
  29. Mattaj, I.W. and L. Englmeier, Nucleocytoplasmic transport: the soluble phase. *Annu Rev Biochem*, 1998. 67: p. 265-306.
  30. Takeda, S. and D.B. McKay, Kinetics of peptide binding to the bovine 70 kDa heat shock cognate protein, a molecular chaperone. *Biochemistry*, 1996. 35(14): p. 4636-4644.
  31. Neeffjes, J.J., F. Momburg, and G.J. Hammerling, Selective and ATP-dependent translocation of peptides by the MHC-encoded transporter. *Science*, 1993. 261(5122): p. 769-771.
  32. Villanueva, M.S., et al., Efficiency of MHC class I antigen processing: a quantitative analysis. *Immunity*, 1994. 1(6): p. 479-489.
  33. Benham, A.M. and J.J. Neeffjes, Proteasome activity limits the assembly of MHC class I molecules after IFN-gamma stimulation. *J Immunol*, 1997. 159(12): p. 5896-5904.
  34. Cascio, P., et al., 26S proteasomes and immunoproteasomes produce mainly N-extended versions of an antigenic peptide. *EMBO J*, 2001. 20(10): p. 2357-2366.
  35. Fruci, D., et al., Efficient MHC class I-independent amino-terminal trimming of epitope precursor peptides in the endoplasmic reticulum. *Immunity*, 2001. 15(3): p. 467-476.
  36. Basu, S., et al., CD91 is a common receptor for heat shock proteins gp96, hsp90, hsp70, and calreticulin. *Immunity*, 2001. 14(3): p. 303-313.
  37. Wallner, B.P., et al., Isolation of bovine kidney leucine aminopeptidase cDNA: comparison with the lens enzyme and tissue-specific expression of two mRNAs. *Biochemistry*, 1993. 32(36): p. 9296-301.
  38. Gurdon, J.B., G.A. Partington, and E.M. De Robertis, Injected nuclei in frog oocytes: RNA synthesis and protein exchange. *J Embryol Exp Morphol*, 1976. 36(3): p. 541-553.



